BES Analysis Memo

J/ψ and ψ' decays to Axialvector plus Pseudoscalar Mesons

Stephen L. Olsen
University of Hawaii

-ABSTRACT-

We report the status of an analysis of decays $\psi' \to AP$, where A and P are conjugate members of the lowest lying axialvector and pseudoscalar meson octets. We find strong signals for $\psi' \to b_1^+(1235)\pi^-$ and $K_1^+(1270)K^-$ but only an upper limit for $K_1^+(1400)K^-$, in contradiction to expectations from flavor-SU(3) symmetry. The branching fraction for $\psi' \to b_1^+(1235)\pi^-$ is found to be consistent with 14%-rule extrapolations from the PDG value for the J/ψ. In the absence of any PDG entries for $J/\psi \to K_1\overline{K}$ decays, we performed a first measurement using a sample of J/ψ's produced via the cascade decay $\psi' \to \pi^+\pi^-J/\psi$. We find an upper limit for the $J/\psi \to K_1^+(1270)K^-$ decay branching ratio that is well below the 14%-rule extrapolation of our ψ' measurement. In addition, the $J/\psi \to K_1\overline{K}$ decays exhibit a flavor-SU(3) violation that is opposite to that seen for the ψ': the branching fraction for $J/\psi \to K_1(1400)\overline{K}$ decays exceeds that for $J/\psi \to K_1(1270)\overline{K}$. This behavior cannot be accommodated by an adjustment to the singlet-triplet axialvector mixing angle.

1 Motivation

1.1 The 14% rule for hadronic ψ' decays

The hadronic decays of both the J/ψ and the ψ' are expected to proceed primarily via an annihilation into three gluons followed by the hadronization of these gluons into physically observable hadrons. The similarity between the parton-level final states has led to the conjecture that ratio of the J/ψ and ψ' decay branching fractions into any exclusive final state X_h is given by the ratio of the square of the wave function at the origin of the constituent $c\bar{c}$ quark state, which is well determined from the dilepton decay rates:

$$\frac{Br(\psi' \to X_h)}{Br(J/\psi \to X_h)} = \frac{Br(\psi' \to e^+e^-)}{Br(J/\psi \to e^+e^-)} = 0.147 \pm 0.023. \qquad (1)$$

This conjecture is sometimes referred to as the *the 14% rule.* Although this conjecture seems to work reasonably well for a number of decay channels, it fails badly in ψ' decays to two-body vector- and pseudoscalar-meson (VP) and vector- and tensor-meson (VT) final states.

1.1.1 $\psi' \to VP$ and VT decays

The MARK II collaboration reported in 1983 that the $\rho\pi$ and $K^*(890)\overline{K}$ final states, two important hadronic decay modes of the J/ψ, were not observed in ψ' decays [1]. Subsequently, the BES collaboration has reported that the suppression of the $\rho\pi$ and $K^*\overline{K}$ decays of the ψ' decays is quite severe: upper limits for the two modes correspond to supressions relative to 14%-rule expectations by factors of more than 50 and 30, respectively [2]. In addition, the BES group has found suppressions in the VT final states: the decays $\psi' \to K^*\overline{K_2^*}$, ρa_2, and ωf_2 are found to be suppressed by at least a factor of five [3]. To date, no convincing evidence has been uncovered for hadronic ψ' decays that are enhanced relative to 14%-rule expectations.

1.2 The axialvector meson octets

There are two lowest-lying axialvector-meson octets. These correspond to the singlet ($^1P_1$) and triplet ($^3P_1$) spin states of two quarks in a p-wave orbital angular momentum state. The non-strange, $I = 1$ members of the two octets have opposite G-parity: the $b_1(1235)$ is in the $^1P_1$ octet and has $G = +1$, while the $a_1(1260)$ is in the $^3P_1$ octet and has $G = -1$. The strong decays of the J/ψ and ψ' conserve G-parity: the axialvector pseudoscalar (AP) decays $b_1\pi$ are G-parity allowed and are seen in J/ψ decays; the $a_1\pi$ decays are G-parity forbidden and are not seen in J/ψ decays.

1.2.1 The strange axialvector mesons

Since the strange members of the two $^3P_1$ and $^1P_1$ octets, called the K_A and K_B, respectively, do not have definite C-parity, the observed physical states are mixtures of the K_A and K_B quark states. These are identified with the $K_1(1270)$ and the $K_1(1400)$ meson states:

$$K_1(1270) = \cos\theta K_B + \sin\theta K_A \quad (2)$$

$$K_1(1400) = \cos\theta K_A - \sin\theta K_B, \quad (3)$$

where the mixing angle is near $\theta = 45^0$ [4]. The dominant $K_1(1270)$ decay mode are to $K\rho$ (Br = 42%) and $K_2^*(1430)\pi$ (Br=28%) and, since the resonance mass $M_{K_1(1270)} = 1.270 \pm 0.010$ GeV is nearly the same as $M_K + M_\rho$ and well below $M_{K_2(1430)} + M_\pi$, significant phase space distortions of the line shape are expected. The $K_1(1400)$ decays almost always to $K^*\pi$ (Br = 92%).

To the extent that flavor-SU(3) is a good symmetry, the amplitude for two body decays to conjugate mesons in the same pair of octets should be equal. Thus, since the $J/\psi(\psi') \to a_1\pi$ decays are forbidden by G-parity, the $J/\psi(\psi') \to K_A\overline{K}$ decays are disallowed and one expects relatively pure $K_B\overline{K}$ final states in J/ψ and ψ' decays. In that case, since

$$K_B = \cos\theta K_1(1270) - \sin\theta K_1(1400), \tag{4}$$

with $\theta \simeq 45^0$, there should be roughly equal amounts of $K_1(1270)$ and $K_1(1400$.)

1.3 Expectations

The PDG value for the $J/\psi \to b_1^+(1235)\pi^- + \mathrm{cc}$ branching ratio is $(3.0 \pm 0.5) \times 10^{-3}$ [5]. There is no PDG entry for the ψ' for this mode. Applying the 14% rule gives the expectation $Br(\psi' \to b_1^+(1235)\pi^- + cc) \simeq 4.4 \times 10^{-4}$. Since the decay $b_1 \to \omega\pi$ is dominant, we search for $b_1^+\pi^-$ decays in the $\psi' \to 2(\pi^+\pi^-)\pi^0$ event sample, where one $\pi^+\pi^-\pi^0$ combination forms an ω. The $b_1^0\pi^0$ decay mode has two π^0's in the final state. These are difficult for the BES detector and are not considered here.

We search for $\psi' \to K_1^+K^-$ decays where the K_1 decays via $K_1^+ \to K^+\pi^+\pi^-$ in the $\psi' \to K^+K^-\pi^+\pi^-$ event sample. Since there are no PDG entries for either the J/ψ or ψ' decays to $K_1\overline{K}$, we search for $J/\psi \to K_1^+K^-$ decays using a sample of J/ψ produced by the cascade decay $\psi' \to \pi^+\pi^-J/\psi$; $J/\psi \to K^+K^-\pi^+\pi^-$.

2 The BES detector

This analysis is based on a sample of 3.4 million $e^+e^- \to \psi'$ events collected in the BES detector at the BEPC storage ring of the Institute of High Energy Physics in Beijing. The BES detector is described in some detail in ref. [6]. The features that are most important for the analysis reported here are the 40-layer main cylindrical drift chamber (MDC), the 48-scintillation counter time-of-flight (TOF) system, and the 12-layer lead-gas barrel electromagnetic shower counter (BSC). These are all situated in a 0.45 T solenoidal magnetic field. Charged particle track trajectories are measured in the MDC with a momentum resolution of 2.1% $\sqrt{1+p^2(GeV)}$. The directions and energies of high energy γ-rays are measured in the BSC with angular and energy resolutions of $\sigma_{\phi,\theta} \simeq 5$ mrad and $\sigma_E/E = 0.22/\sqrt{E(GeV)}$, respectively. Particle identification is provided by drift chamber dE/dx measurements and particle velocities as determined from the TOF system. Tracks with $|\cos\theta| \leq 0.75$ traverse all 40 layers of the MDC and are well contained in the TOF and BSC detectors. In the events used for the analyses reported here, all of the produced particles of the event being studied are required to be detected. The particle momentum measurements and identification assignments are further refined by the application of four- and five-constraint kinematic fits.

3 Determination of $Br(\psi' \to b_1^+(1235)\pi^- \ + \ cc)$

The branching ratio for $b_1(1235) \to \omega(780)\pi$ is very nearly 100% and we concentrate on events where the ω decays via $\omega(780) \to \pi^+\pi^-\pi^0$ which has a BR of 88.8%. The events of interest have a topology of

$$\psi' \to \pi^+\pi^-\pi^+\pi^-\gamma\gamma, \tag{5}$$

where the invariant mass of the two $\gamma' s$ has the value $M_{\gamma\gamma} = M_{\pi 0}$.

3.1 $\psi' \to \pi^+\pi^-\pi^+\pi^-\pi^0$ preselection

We select events with four charged tracks in the polar angle region $|\cos\theta| \leq 0.74$ and with zero net charge. In addition we require two or more neutral BSC energy clusters that each have: $|\cos\theta| \leq 0.75$; $E_{BSC} \geq 50$ MeV; and $\theta_{open} \geq 26^0$, where θ_{open} is the angle between the γ and the nearest charged track (at the production point). The four charged tracks and each $\gamma\gamma$ pairing are required to satisfy a 5-constraint kinematic fit to the $\psi' \to \pi^+\pi^-\pi^+\pi^-\pi^0$ hypothesis with $\chi^2 \leq 50$. For events with more than two $\gamma' s$, the pairing with the best χ^2 is accepted and the unpaired $\gamma' s$ are ignored.

Approximately half of the surviving events correspond to $\psi' \to \pi^+\pi^- J/\psi$ followed by $J/\psi \to \rho\pi$ decays. These events are eliminated by requiring the missing mass recoiling against any (of the four possible) $\pi^+\pi^-$ pair to be outside the range $M_{J/\psi} \pm 50$ MeV. The 2505 surviving event candidates are written to an Ntuple file for subsequent analysis.

3.2 $\psi' \to \pi^+\pi^-\pi^+\pi^-\pi^0$ selection

The following selection criteria are applied to extract the final sample of $\psi' \to b_1\pi$ event candidates:

$M_{\gamma\gamma}^{prefit} \leq 0.4$ GeV: Figure 1a shows the distribution of prefit values of $M_{\gamma\gamma}$ for the events that survive the preselection. This cut eliminates most of the small tail that extends almost to 1.0 GeV.

$M_{\pi^+\pi^-} \leq 2.9$ GeV: Figure 1b shows the distribution of the invariant mass of the highest momentum π^+ and π^- tracks in the event. The peak near $M_{\pi^+\pi^-} = 3.1$ GeV correspond to events of the type $\psi' \to \eta J/\psi$ with $J/\psi \to \mu^+\mu^-$ or e^+e^- and $\eta \to \pi^+\pi^-\pi^0$. This cut eliminates these events with no loss of $b_1\pi$ signal.

$X_{\pi k}^{\pi^+\pi^-} < 0.9$: Figures 1c-f show the $X_{\pi k}$ distribution for each of the four tracks in the event, ordered according to track momentum and charge (c: the highest momentum negative track, d: the highest momentum positive track, etc.). Here

$$X_{\pi k} = \frac{weight_k}{weight_\pi + weight_k} \tag{6}$$

where $weight_i$ the values assigned by the particle identification system (pid) to the hypothesis $i = \pi$ or k. This eliminates events where the pid unambiguously identifies a particle as a kaon.

$\chi^2_{5c} \leq 20$: Figures 1g shows the χ^2 distribution for the remaining events. We select events with $\chi^2 < 20$, leaving a final selected event sample of 964 events.

3.3 $\psi' \to \pi^+\pi^-\pi^+\pi^-\pi^0$ invariant mass distributions

Figure 2a shows a scatterplot of $\pi^+\pi^-\pi^0$ (vertical) vs $\pi^+\pi^-\pi^\pm\pi^0$ (horizontal) masses for the selected events. There are eight entries per event. The $\omega(780)$ shows up as a horizontal band near the bottom of the scatterplot and there is a clustering in this band at low $\pi^+\pi^-\pi^\pm\pi^0$ masses, indicating the presence of a b_1 signal.

Figures 2b and c show the respective vertical and horizontal projections of the scatterplot. (Each plot has four entries/event). The $\omega(780)$ shows up as an obvious peak in the $\pi^+\pi^-\pi^0$ mass distribution (Fig. 2b); the $b_1(1235)$ is also visible as a small peak in the $\pi^+\pi^-\pi^\pm\pi^0$ mass distribution (Fig. 2c).

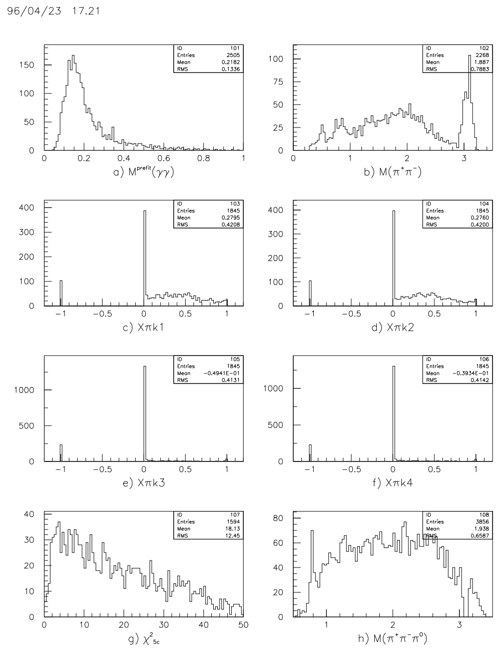

Figure 1: Distributions of precut values of the variables used for the final selection.

Figure 2d shows the $\pi^+\pi^-\pi^0$ mass distribution when one of the $\pi^+\pi^-\pi^\pm\pi^0$ mass combinations is consistent with that of the $\omega(780)$; i.e. $\mid M_{\pi^+\pi^-\pi^0} - 0.782 \mid \leq 0.06$ GeV. Here there is a clear $b_1(1235)$ signal near $M_{\pi^+\pi^-\pi^\pm\pi^0} \simeq 1.23$ GeV. We use fits to this distribution to determine the number of $\psi' \to b_1\pi$ events in our data sample.

3.4 Fits to the $\omega(780)\pi^\pm$ mass distribution.

We fit the $\omega(780)\pi^\pm$ mass distribution shown in Fig. 2d to an s-wave Breit Wigner function with the resonance mass and width fixed at the PDG values for the b_1, of $M_0 = 1.232$ and $\Gamma_0 = 0.155$ GeV. We fit the background under this peak using two different procedures:

i In one procedure we add to the resonance Breit Wigner a smooth curve of the form

$$\begin{aligned} f_{bkg}(Q) &= p_1(Q^{\frac{1}{2}} + p_2 Q^{3/2} + p_3 Q^{5/2}) \quad Q > 0 \\ &= 0 \quad\quad\quad\quad\quad\quad\quad\quad\quad\quad\quad\quad\quad Q \leq 0, \end{aligned} \tag{7}$$

where $Q \equiv M - (M_\pi + M_\omega)$. This function is used to fit the entire mass distribution. The result of this fit, shown in Fig. 3, gives $N_{evt}^{b_1} = 59.2 \pm 13.1$.

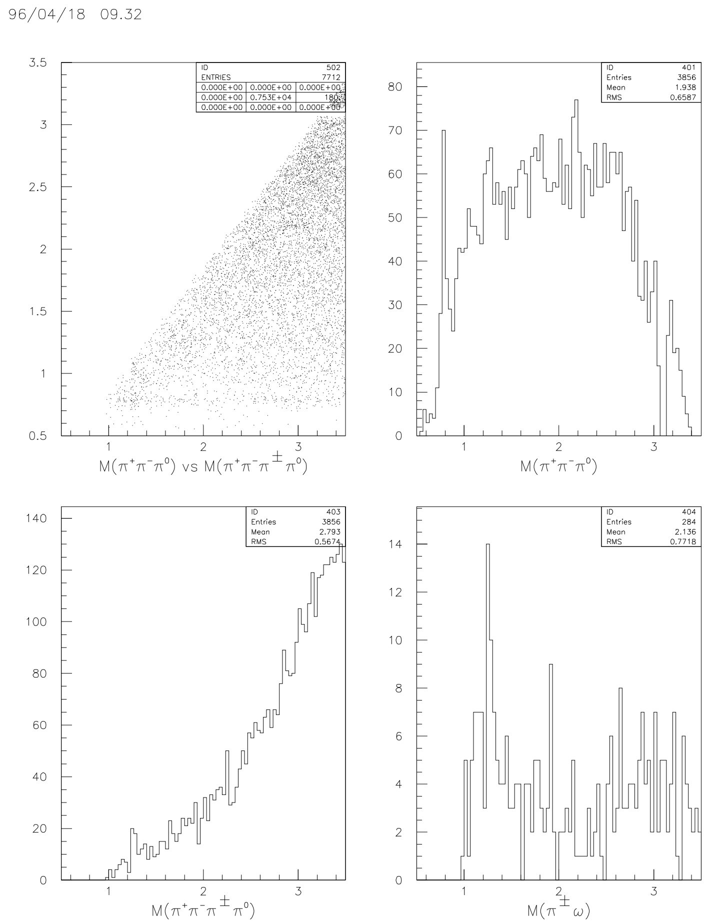

Figure 2: **a)** A scatterplot of $M_{\pi^+\pi^-\pi^0}$ (vertical) vs $M_{\pi^+\pi^-\pi^\pm\pi^0}$ (horizontal) for selected events. **b)** The vertical and **c)** horizontal projections of the scatterplot. **d)** The $\omega\pi^\pm$ mass distribution.

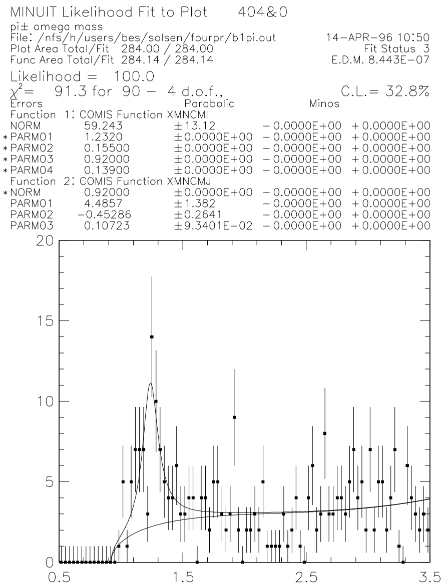

Figure 3: Fit to the $\omega\pi^{\pm}$ mass distribution using f_{bkg} to parameterize the background under the $b_1(1235)$ peak.

ii In the other procedure we attribute all of the events for $M \leq 1.9$ GeV to the b_1 and a second resonance with mass $M \sim 1.7$ and $\Gamma \sim 0.3$ GeV, which could be the $\rho(1700)$ and/or the ρ_3 (1690). The fit is applied only for $\omega\pi$ masses below 1.9 GeV and the mass and width of the second Breit Wigner resonance are allowed to vary. In this case the only background under the b_1 peak is the tail of this second resonance. This gives $N_{evt}^{b_1} = 85.9 \pm 13.2$ and the fit curve shown in Fig. 4.

We expect that the first procedure *overestimates* the background while the second fit *underestimates* it. For the branching ratio determination we use the average of these two results:

$$N_{evt}(\psi' \rightarrow b_1^+\pi^- \ + \ cc) = 72.6 \pm 8.5 \pm 13.3, \tag{8}$$

where the first error is statistical and the second error is the difference between the average and the values from the fits, which is taken as the systematic error associated with uncertainties in the background shape.

3.5 $\psi' \rightarrow b_1^+\pi^-$ acceptance

The detector acceptance and the efficiency for the analysis cuts are evaluated by means of a sample of simulated Monte Carlo events. We generated 5000 $\psi' \rightarrow b_1^+\pi^-$ with subsequent $b_1^+ \rightarrow \omega\pi^+$ decays with flat $\cos\theta$ distributions and $\omega \rightarrow \pi^+\pi^-\pi^0$ final states that

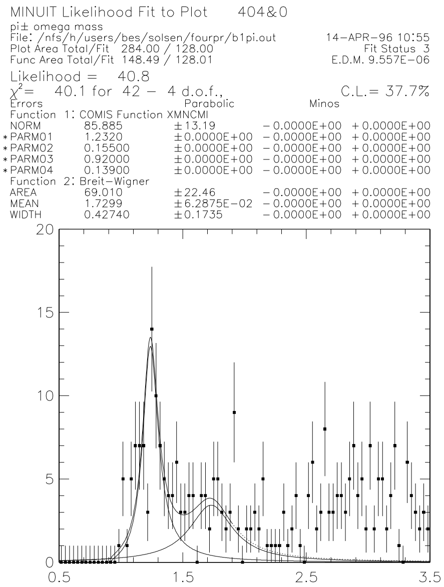

Figure 4: Fit to the $\omega\pi^{\pm}$ mass distribution where the background under the $b_1(1235)$ peak is attributed to a resonance with $M \sim 1.7$ GeV.

uniformly populate phase space. The generated events were passed through a Monte Carlo simulation of the BES detector that generates simulated detector responses. The simulated data are analyzed with the same programs that are used for the data.

The effects of the various selection cuts on the data and the simulated event sample is summarized in Table 1. A fit (see Fig. 5) to the $\omega\pi^+$ mass plot for the surviving 159 events using the same s-wave breit-wigner function gives $N_{evt}^{MC} = 180.7 \pm 13.1$ events, giving an acceptance of $\eta = 0.036 \pm 0.003$. The excess events correspond to those events where more than one $\pi^+\pi^-\pi^0$ combination has a mass in the $\omega(780)$ band.

3.6 The $\psi' \rightarrow b_1^+\pi^-$ branching ratio

We determine the $\psi' \rightarrow b_1^+\pi^-$ (+ cc) branching ratio from the relation

$$Br(\psi' \rightarrow b_1^+\pi^- \ + \ cc) = \frac{N_{evts}}{N_{\psi'}\eta \ Br(b_1^+ \rightarrow \omega\pi^+)Br(\omega \rightarrow \pi^+\pi^-\pi^0)}, \tag{9}$$

where $N_{evts} = 72.6 \pm 8.5 \pm 13.3$ is the number of b_1 events, $\eta = 0.036 \pm 0.003$ is the acceptance, $N_{\psi'} = (3.44 \pm 0.31) \times 10^6$ is the number of $\psi's$ in the events sample [7], and the branching ratios $Br(b_1^+ \rightarrow \omega\pi^+) = 1.0$ and $Br(\omega \rightarrow \pi^+\pi^-\pi^0) = 0.888 \pm 0.006$ are taken from the PDG tables [5]. The result is

$$Br(\psi' \rightarrow b_1^+\pi^- \ + \ cc) = (6.6 \pm 0.8 \pm 1.4) \times 10^{-4}, \tag{10}$$

Table 1: A tabulation of the $b_1\pi$ selection cuts.

Numbers of events surviving each requirement

	94 data	95 data	Simulated events
Preselection:			
Generated			5000
4 chrgd trks			
$\sum q = 0$			
$n_\gamma \geq 2$	258100	475032	1856
$\lvert\cos\theta_{chg}\rvert \leq 0.74$	136899	253248	1089
$E_\gamma > 0.5$ GeV			
$\lvert\cos\theta_\gamma\rvert \leq 0.75$			
$\theta_{open} > 16^o$	114008	208883	420
$\chi^2_{5c} \leq 50$	1699	3137	193
Selection:			
$\lvert M_{\pi^+\pi^-recoil} - m_{J/\psi}\rvert \geq 0.05$ GeV	882	1623	174
$M^{prefit}_{\gamma\gamma} < 0.4$ GeV	1466	802	172
$M_{\pi^+\pi^-} < 2.9$ GeV	1205	640	171
$X_{\pi K} < 0.9$	1041	553	171
$\chi^2_{5c} \leq 20$	628	336	159
Mass cuts:			
$\lvert M_{\pi^+\pi^-\pi^O} - m_\omega\rvert \leq 0.06$GeV	142	86	171

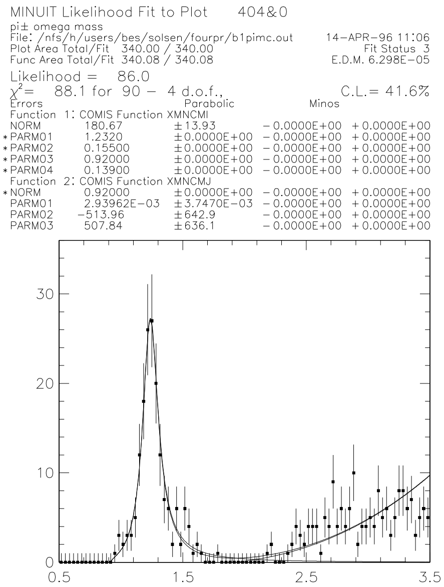

Figure 5: Fit to the $\omega\pi^{\pm}$ mass distribution for Monte Carlo events that survive the event selection.

where the second error is the systematic error that is dominated by the uncertainty in the background subtraction. This is the first measurement of this branching fraction for the ψ' and is about 1.3 standard deviations above the 14% rule expectations applied to the PDG result for the J/ψ.

4 $\psi' \to K_1(1270)K$ and $K_1(1400)K$

The $K\rho$ channel is the dominant $K_1(1270)$ decay mode, with a branching fraction of $42 \pm 6\%$ [5]. The ispin decomposition of the $(K\rho)^+$ final state is:

$$(K\rho)^+ = \sqrt{\frac{2}{3}}K^0\rho^+ - \sqrt{\frac{1}{3}}K^+\rho^0 \tag{11}$$

The branching ratio for $\rho^0 \to \pi^+\pi^-$ is essentially 100%.

The $K^*\pi$ channel is the dominant decay mode for the $K_1(1400)$ with a branching fraction of 94$\pm$ 6%. It is also significant for the $K_1(1270)$ where the $Br(K_1(1270) \to K^*\pi) = 16 \pm 6\%$ and the $Br(K_1(1270) \to K_2^*(1430)\pi) = 28 \pm 4\%$. The decays $K_2^*(1430) \to K\pi$, which has a branching ratio of $49.7 \pm 1.2\%$ [5], contribute to the $\psi' \to K^+K^-\pi^+\pi^-$ final states that are studied here The ispin decomposition of the

$(K*\pi)^+$ final state is

$$(K^*\pi)^+ = \sqrt{\frac{2}{3}}K^{*0}\pi^+ - \sqrt{\frac{1}{3}}K^{*+}\pi^0 \qquad (12)$$

with

$$K^{*0} = \sqrt{\frac{1}{3}}K^0\pi^0 - \sqrt{\frac{2}{3}}K^+\pi^- \qquad (13)$$

$$K^{*+} = \sqrt{\frac{2}{3}}K^0\pi^+ - \sqrt{\frac{1}{3}}K^+\pi^0, \qquad (14)$$

In this analysis we consider $\psi' \to K^+K^-\pi^+\pi^-$ final states. The relevant final states and branching fractions that take the appropriate Clebsch-Gordon coefficients into account are as follows:

$$\begin{array}{lllllllll}
\psi' & \to & K_1^+(1270)K^- & \to & K^+\rho^o K^- & \to & K^+K^-\pi^+\pi^- & = & 0.19 \pm 0.02 \\
 & & & \to & K^{*0}\pi^+K^- & \to & K^+K^-\pi^+\pi^- & = & 0.13 \pm 0.02 \\
 & \to & K_1^+(1400)K^- & \to & K^{*0}\pi^+K^- & \to & K^+K^-\pi^+\pi^- & = & 0.41 \pm 0.02
\end{array}$$

4.1 $\psi' \to K^+K^-\pi^+\pi^-$ event selection

4.1.1 Preselection

We select events with four charged tracks in the polar angle region $|\cos\theta| \leq 0.74$ and with zero net charge. To reduce the number of $\psi' \to \pi^+\pi^- J/\psi$ cascade events where $J/\psi \to \ell^+\ell^-$, we veto events where both the highest momentum positive and negative tracks are identified as muons or where they *both* have a BSC energy deposit that is greater than 0.8 GeV.

The four charged tracks are subjected to a 4-constraint kinematic fit to the $\psi' \to K+K^-\pi^+\pi^-$ hypothesis for each of the four possible particle assignment combinations and select the assignment with the best χ^2 value. We keep the 8256 events with $\chi^2 \leq 50$ and write them into a Ntuple file for further analysis. Included in the Ntuple file is the χ^2 value returned from a 4-c fit to the hypothesis $\psi' \to \mu^+\mu^-\pi^+\pi^-$, where the highest momentum positive and negative tracks are taken to be the μ^+ and μ^-.

4.1.2 Final selection

The following selection criteria are applied to extract the final sample of $\psi' \to K_1^+K^-$ event candidates:

$\chi^2_{\mu^+\mu^-\pi^+\pi^-} > \chi^2_{K^+K^-\pi^+\pi^-}$: Figure 6a shows the distribution of χ^2 values for the fit of the events to the $\psi' \to \mu^+\mu^-\pi^+\pi^-$ hypothesis. We reject events where this fit is better than the $K^+K^-\pi^+\pi^-$ fit.

$\chi^2_{K^+K^-\pi^+\pi^-} < 12.$: Figure 6b shows the distribution of χ^2values for the $K^+K^-\pi^+\pi^-$ hypothesis. We keep events with $\chi^2 < 12$.

$M_{\pi^+\pi^-} \leq 2.4$ GeV : Figure 6c shows the distribution of the invariant mass of the tracks assigned as the π^+ and π^-. The peak near $M_{\pi^+\pi^-} = 2.4$ GeV correspond to events of the type $\psi' \to \pi^+\pi^- J/\psi$; with $J/\psi \to p\bar{p}$ where the cascade pions are misassigned as kaons and the $p\bar{p}$ are misassigned as pions. This cut eliminates these events with essentially no loss of $K_1\overline{K}$ signal.

$1.05 \leq M_{K^+K^-} 3.0$ GeV : Figure 6d shows the distribution of the invariant mass of the tracks assigned as the K^+ and K^-. The peak near $M_{K^+K^-} = 3.1$ GeV correspond to events of the type $\psi' \to \pi^+\pi^- J/\psi$ where the J/ψ decays to two charged tracks. (This peak correlates with the low mass peak in the $M_{\pi^+\pi^-}$ distribution shown in Fig. 6c.) Not as clear in this plot is a small peak at low K^+K^- masses corresponding to $\phi \to K^+K^-$. This cut eliminates these events with a little loss of $K_1\overline{K}$ signal.

$\mid X^{K^\pm}_{\pi k} \mid > 0.1$: Figures 6e and f show the $X_{\pi k}$ distribution for the tracks assigned as the K^- and K^+, respectively. Here

$$X_{\pi k} = \frac{weight_k}{weight_\pi + weight_k}, \tag{15}$$

where $weight_i$ the values assigned by the particle identification system (pid) to the hypothesis $i = \pi$ or K. This eliminates events where the pid unambiguously identifies as a pion a particle that the 5-c fit assigned as a kaon.

A total of 445 events satisfy these selection requirements.

4.2 $\psi' \to K^+K^-\pi^+\pi^-$ invariant mass distributions

Figure 7a shows a scatterplot of $\pi^+\pi^-$ (vertical) $K^\pm\pi^+\pi^-$ (horizontal) masses for the selected events (two entries per event). The $\rho(770)$ shows up as a horizontal band in the scatterplot; a clustering of events at the left edge of this band indicates the presence of a $K_1(1270)$ signal. Figure 7b shows the $\pi^+\pi^-$ mass distribution. The $\rho(770)$ shows

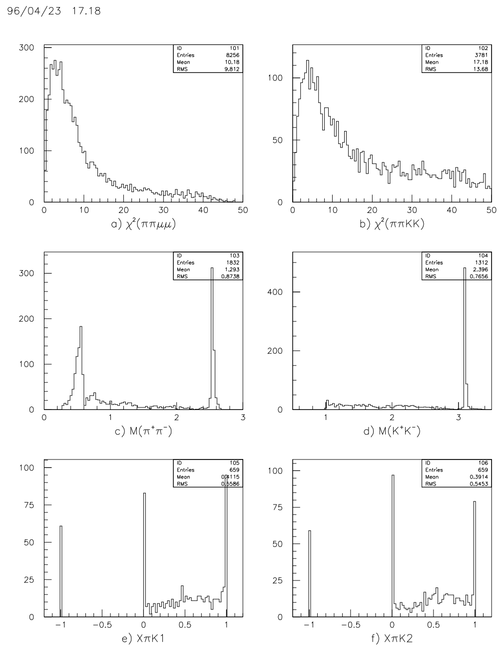

Figure 6: Distributions of precut values of the variables used for the $\psi' \to K^+K^-\pi^+\pi^-$ selection.

up as an obvious peak. Figure 7c shows the $K^\pm\rho^0$ mass distribution, where the ρ^0 is taken to be $\pi^+\pi^-$ pairs within ± 0.150 GeV of the nominal ρ mass. A peak at low $M_{K\rho}$ values is prominent.

Figure 7d shows a scatterplot of $K^\pm\pi^\mp$ (vertical) vs $K^\pm\pi^+\pi^-$ (horizontal) masses for the selected events (four entries/event). The $K^*(890)$ shows up as a horizontal band. Figure 7e shows the $K^\pm\pi^\mp$ mass distribution (two entries/event) where the $K^*(890)$ shows up as an obvious peak. Figure 7f shows the $K^{*0}\pi^\pm$ mass distribution, where the K^* is taken to be $K^\pm\pi^\mp$ pairs within ± 0.050 GeV of the nominal K^{*0} mass. There is some peaking of events near low M_K values. There is not much evidence for the $K_1(1400)$, even though the $K^*\pi$ channel is its dominant decay mode.

4.3 Fits to the $K^\pm\rho$ mass distributions.

As noted above, the restricted phase space for the $K_1(1270) \to K\rho$ decay is expected to distort the resonance shape for this mode. We, therefore, fit the $K^\pm\rho$ mass distribution of Fig. 7c to specially devised function $f_{K\rho}$ that explicitly takes these distortions into account [8]. This function is the convolution an s-wave Breit Wigner function with

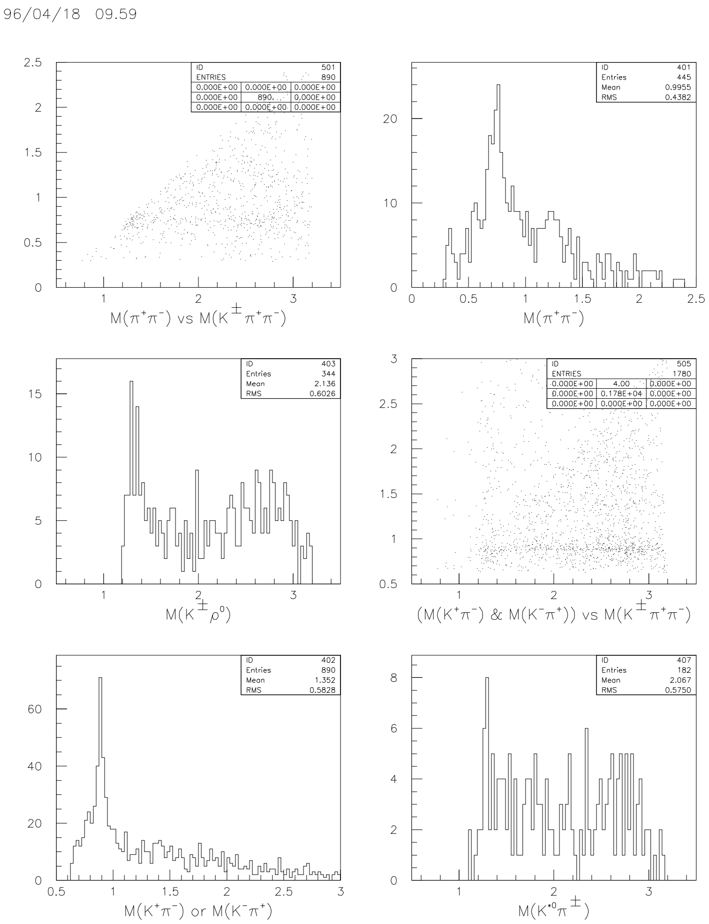

Figure 7: **a)** A scatterplot of $\pi^+\pi^-$ (vertical) vs $K^\pm\pi^+\pi^-$ (horizontal) masses for selected events. The **b)** $\pi^+\pi^-$ and **c)** K_ρ mass distributions. **d)** A scatterplot of $K^\pm\pi^\mp$ (vertical) vs $K^\pm\pi^+\pi^-$ (horizontal) masses for selected events. The **e)** $K\pi$ and **f)** $K^*\pi$ mass distributions.

mass and width fixed at the PDG values for the $K_1(1270)$ ($M_{K1} = 1.270$ GeV and $\Gamma_{K1} = 0.090$ GeV) with a p-wave ρ meson Breit Wigner with $M_\rho = 0.77$ GeV and $\Gamma_\rho = 0.150$ GeV. Specifically,

$$f_{K\rho}(M_{K\pi\pi}) = \frac{Aq^*_{K\pi\pi}}{(M^2_{K1} - M^2_{K\pi\pi})^2 + M^2_{K1}\Gamma^2_{K1}} \int_{M^{min}_{\pi\pi}}^{M^{max}_{\pi\pi}} \frac{q^*_K (q^*_\pi/q^0_\pi)^3 \Theta(M_{K\pi\pi} - M_K - M_{\pi\pi}) dM_{\pi\pi}}{(M^2_\rho - M^2_{\pi\pi})^2 + M^2_\rho [\Gamma_\rho (q^*_\pi/q^0_\pi)^3]^2} \tag{16}$$

where:

$q^*_{K\pi\pi}$ is the momentum of the $K\pi\pi$ system in the ψ' rest frame;

$M^{min}_{\pi\pi}$ and $M^{max}_{\pi\pi}$ are the lower and upper limits of the ρ mass selection;

q^*_K is the momentum of the K in the $K\pi\pi$ rest frame;

q^*_π is the π momentum in the $\pi\pi$ rest frame; and

q^0_π is the π momentum in the $\pi\pi$ rest frame for $M_{\pi\pi} = M_\rho$.

Given the mass cuts listed above, the only free parameter for this function is the overall normalization.

For the background under the peak we employ the same two procedures that were used for the b, analysis and are described above in Section 3.4. Figure 8 shows the results of a fit of the function $f_{K\rho} + f_{bkg}$ to the whole $K\rho$ mass distribution of Fig. 4.3c. The number of K_1, (1270) events from this fit is 65.7 ± 12.7. Figure 9 shows the results of a fit of the function $f_{K\rho}$ plus a Breit Wigner with a starting mass of 1.7 GeV and width of 0.25 GeV to the K_ρ mass distribution below 1.9 GeV. This could be the $K^*(1680)$ the octet partner of the $\rho(1700)$. This fit gives 85.8 ± 12.0 $K_1(1270)$ events. We consider the fits as under and overestimates to the background and take the average value as the measured number of events and the difference from the average as the systematic error associated with uncertainties in the background under the $K_1(1270)$ peak:

$$N^{(1270)}_{evts} = 75.8 \pm 8.7 \pm 10.2 \tag{17}$$

4.4 Fits to the $K^*\pi$ mass distributions.

We fit the region $K^{*0}\pi^\pm$ mass distribution (Fig. 7f) below 1.9 GeV to $f_K\rho$ plus an s-wave Breit Wigner with mass and width fixed at the PDG values for the K_1 (1400) ($m_{K1} = 1.40$ GeV and $\Gamma_{K1} = 0.173$ GeV) and an additional Breit Wigner with mass

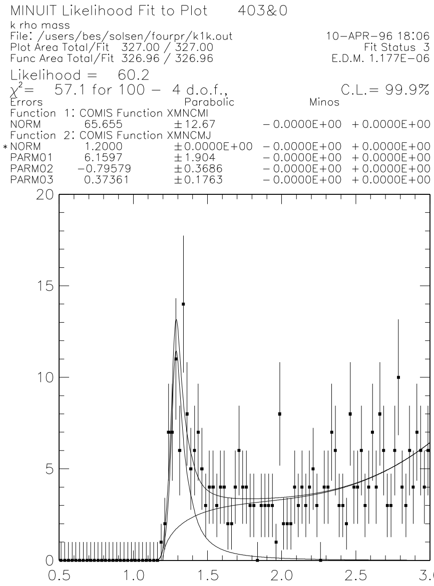

Figure 8: Fit to the $K^+\rho^0$ mass distribution using the function $f_{K\rho}$ for the K_1(1270 line shape and f_{bkg} to parameterize the background.

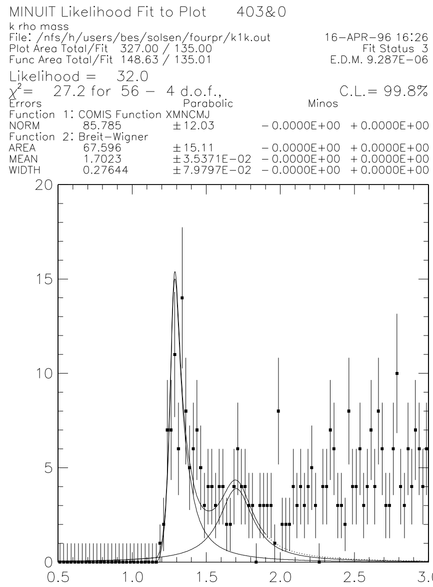

Figure 9: Fit to the $K^+\rho^0$ mass distribution using a Breit Wigner resonance with mass near 1.7 and width near 0.25 GeV as an estimate for the background under the $K_1(1270)$ peak.

near 1.7 and width near 0.25 GeV. The mass and width of this last Breit Wigner is allowed to vary. The resulting fit, shown in Fig. 10, gives 27.9 $\pm$11.2 $K_1(1400)$ events. Since the mass distribution can be fit without any $K_1(1400)$, we use this number to derive a 90% CL upper limit of $N_{limit}^{(1400)} < 42.2$ (90% CL).

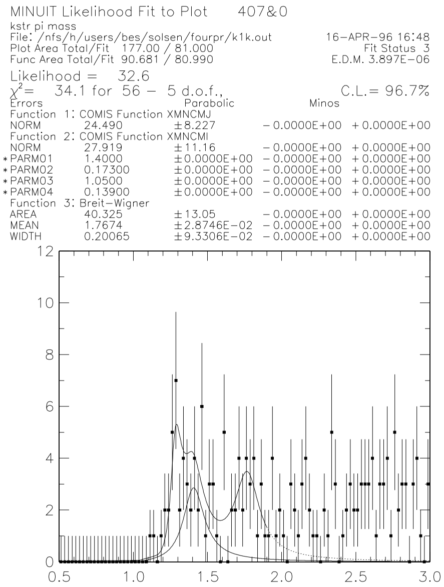

Figure 10: Fit to the $K^{*0}\pi^{\pm}$ mass distribution using a Breit Wigner resonance with mass near 1.7 and width near 0.25 GeV as an estimate for the background under the $K_1(1400)$ peak.

4.5 $\psi' \rightarrow K_1^+ K^-$ acceptance

The detector acceptance and the efficiency for the analysis cuts are evaluated by means of a sample of simulated Monte Carlo events. We generated 5000 $\psi' \rightarrow K_1^+(1270)K^-$ with subsequent $K_1^+(1270) \rightarrow K^+\rho^0$; $\rho^0 \rightarrow \pi^+\pi^-$ decays with flat angular distributions. In addition, we generated 5000 $\psi' \rightarrow K_1^+(1400)K^-$ with subsequent $K_1^+(1400) \rightarrow K^{*0} \rightarrow K^+\pi^-$ decays, also with flat angular distributions. The generated events were passed through a Monte Carlo simulation of the BES detector that generates simulated detector responses. The simulated data are analyzed by the same programs that are used for the data. The $K\rho$ mass distribution for the events in the first sample that survive all the cuts is fit to the same $f_{K\rho}$ function, yielding 635.0 ± 26.1 events, or an acceptance for this mode of $\eta_{K\rho}^{(1270)} = 0.127 \pm 0.005$.

Table 2: A tabulation of the $K_1 K$ selection cuts.

Numbers of events surviving each requirement

	94 data	95 data	Simulated events $K_1(1270) \to K^+\rho^0$	Simulated events $K_1(1400) \to K^{*0}\pi^+$
Preselection:				
Generated			5000	5000
4 chrgd trks			3294	3281
$\sum q = 0$			3103	3119
pass $\mu^+\mu^-$ veto	309068	579202	3095	3112
pass e^+e^- veto	294320	552696	3075	3101
$\lvert\cos\theta_{chg}\rvert \leq 0.74$	154072	291186	1822	1741
$\chi^2_{4c} \leq 50$	2944	5312	1382	1306
Selection:				
$\chi^2_{\mu\mu\pi\pi} > \chi^2_{KK\pi\pi}$	1364	2417	1360	1283
$\chi^2_{KK\pi\pi} \leq 12$	655	1177	1205	1134
$M_{\pi^+\pi^-} < 2.4$ GeV	464	848	1204	1133
$1.05 < M_{K^+K^-} < 3.0$ GeV	239	420	1149	1064
$\lvert X^{K^+K^-}_{\pi K}\rvert > 0.1$	160	285	858	833
Mass cuts:				
$\lvert M_{\pi^+\pi^-} - M_\rho\rvert \leq 0.15$GeV	114	230	612	427
$\lvert M_{K\pi} - M_{K^*}\rvert \leq 0.05$GeV	73	109	263	555

The $K^*\pi$ mass distribution for the surviving events from the second sample are fit to an s-wave Breit Wigner function, yielding 557.3 $\pm$ 24.3 events, corresponding to an acceptance of $\eta^{(1400)}_{K^*\pi} = 0.111 \pm 0.005$. In the $K_1(1400) \to K^*\pi$ MC event sample, 427 events have a $\pi^+\pi^-$ mass that is within ± 0.15 GeV of m_ρ, and pass the $K\rho$ selection requirements. We infer from this an acceptance for $K_1(1270) \to K^*\pi$ decays $\eta^{(1270)}_{K^*\pi} = 0.085 \pm 0.005$. A summary of the effect of the cuts on the real and simulated data is provided in Table 2.

4.6 $\psi' \to K_1(1270)^+K^-$ and $K_1(1400)^+K^-$ branching ratios

Using the relation

$$\begin{aligned} Br(\psi' &\to K_1^+(1270)K^- \ + \ cc) \qquad (18) \\ &= \frac{N_{evts}^{(1270)}}{N_{\psi'}[\eta_{K\rho}^{(1270)} Br_{K_1(1270)\to K\rho\to K^+\pi^+\pi^-} + \eta_{K^*\pi}^{(1270)} Br_{K_1(1270)\to K^*\pi\to K^+\pi^+\pi^-}]} \end{aligned}$$

we determine the branching ratio result

$$Br(\psi' \to K_1^+(1270)K^- \ + \ cc) = (7.6 \pm 0.9 \pm 1.5) \times 10^{-4}. \qquad (19)$$

We establish a 90% CL upper limit for the $\psi' \to K_1(1400)^+K^-$ (+ cc) branching ratio from the relation

$$Br(\psi' \to K_1^+(1400)K^- \ + \ cc) < \frac{N_{limit}^{(1400)}}{N_{\psi'}\eta_{K^*\pi}^{(1400)} Br_{K_1(1400)\to K^*\pi\to K^+\pi^+\pi^-}}, \qquad (20)$$

with the result

$$Br(\psi' \to K_1^+(1400)K^- \ + \ cc) < 2.7 \times 10^{-4} \quad 90\% \text{ CL}. \qquad (21)$$

Contrary to the flavor-SU(3) expectation of equal amounts of $K_1(1270)$ and $K_1(1400)$, the K_1 mode is smaller than the $K_1(1270)K$ mode by at least a factor of three. There are no PDG entries for these modes for the J/ψ for comparison.

5 $J/\psi \to K_1(1270)K$ and $K_1(1400)K$

For the $\psi' \to K_1^+(1270)K^-$, we see a branching ratio of $(7.6 \pm 0.9 \pm 1.5) \times 10^{-4}$, which is quite large for an exclusive hadronic ψ' decay channel. We do not see a comparable signal for $\psi' \to K_1^+(1400)K^-$, although this is what is expected from flavor-SU(3). According to the 14% rule, the corresponding branching fraction for the J/ψ, should be around 0.5%, which would make it one of the most prominent exclusive hadronic decay channels. The absence of any PDG entries for $J/\psi \to K_1(1270)K$ or $K_1(1400)K$ makes one suspicious that this may not be the case. We used the $\psi' \to \pi^+\pi^- J/\psi$ cascade events in our ψ' data sample to make a first measurement of branching ratios for $J/\psi \to K_1(1270)\overline{K}$ and $K_1(1400)\overline{K}$.

5.1 $\psi' \to \pi^+\pi^- J/\psi; J/\psi \to K^+K^-\pi^+\pi^-$ event selection

5.1.1 Preselection

We select events with six charged tracks in the polar angle region $|\cos\theta| \leq 0.74$ and with zero net charge. No criteria is used on the number or quality of neutral tracks. The six tracks are subjected to a 5-constraint kinematic fit to the $\psi' \to \pi^+\pi^- J/\psi; J/\psi \to K + K^-\pi^+\pi^-$ hypothesis where each of nine neutral particle pairs are tried as the K^+ and K^- combination, and the remaining lowest momentum positive and negative tracks are assigned to be the cascade pions. We select the assignment with the best χ^2 value. We keep the 1283 events with $\chi^2 \leq 50$ and write them into a Ntuple file for further analysis.

5.1.2 Final selection

The following selection criteria are applied to extract the final sample of $J/\psi \to K_1^+K^-$ event candidates:

$\chi^2_{5c} < 15.$: Figure 11a shows the distribution of χ^2 values for the $\psi' \to \pi^+\pi^- J/\psi; J/\psi \to K^+K^-\pi^+\pi^-$ hypothesis. We keep events with $\chi^2 < 12$.

$|X_{\pi k}^{K\pm}| > 0.1$: Figures 11b and c show the $X_{\pi k}$ distribution for the tracks assigned as the K^- and K^+, respectively, where $X_{\pi k}$ is the relative K-π weight assigned by the particle identification system. This eliminates events where the pid unambiguously identifies as a pion a particle that the 5-c fit assigned as a kaon.

A total of 383 events satisfy these selection requirements.

5.2 $J/\psi \to K^+K^-\pi^+\pi^-$ invariant mass distributions

Figure 12a shows a scatterplot of $\pi^+\pi^-$ (vertical) $K^\pm\pi^+\pi^-$ (horizontal) masses for the selected events (two entries per event). Figure 12b shows the $\pi^+\pi^-$ mass distribution. There is some sign of a $\rho(770)$ in the $\pi^+\pi^-$ mass histogram, but not much evident clustering of events in the scatterplot. Figure 12c shows the $K^\pm\rho^0$ mass plot, where the ρ^0 is taken to be $\pi^+\pi^-$ pairs within ± 0.150 GeV of the nominal ρ mass. There is not much sign of of a $K_1(1270)$ signal. (The $J/\psi \to K^\pm\rho^0$ distribution of Fig. 12c should be compared with the $\psi' \to K^\pm\rho^0$ distribution of Fig. 7c.) However there are rather distinct peaks near 1.4 and 1.7 GeV. The peak near $M \simeq 1.4$ GeV could be due to the $K_1(1400)$. Even though this resonance decays primarily to $K^*\pi$, the $\pi^+\pi^-$ final

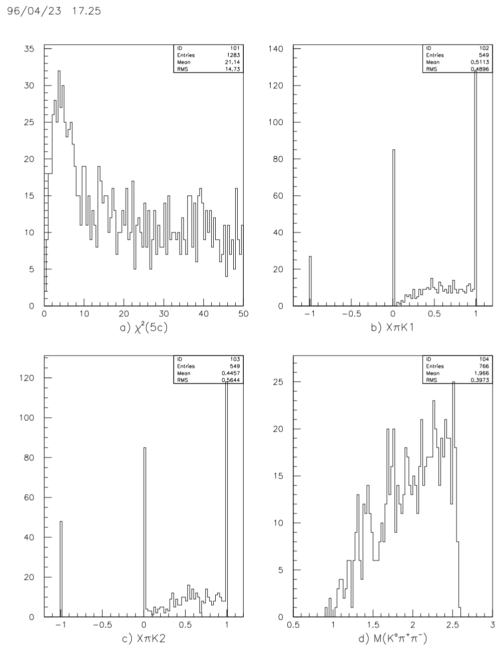

Figure 11: Distributions of precut values of the variables used for the $J/\psi \rightarrow K^+K^-\pi^+\pi^-$ selection.

state frequently has an invariant mass that lies within ρ cut (see below). The peak near $M \simeq 1.7$ GeV may be due to the $K_3^*(1780)$. We discuss this possibility below.

Figure 12d shows a scatterplot of $K^\pm\pi^\mp$ (vertical) vs $K^\pm\pi^+\pi^-$ (horizontal) masses for the selected events (four entries/event). There are two entries per event. Figure 12e shows the $K^\pm\pi^\mp$ mass distribution (two entries/event). Here the $K^*(890)$ is evident both as a horizontal band in the scatterplot and a peak in the $K\pi$ mass histogram. Figure 12f shows the $K^{*0}\pi^\pm$ mass distribution, where the K^* is taken to be $K^\pm\pi^\mp$ pairs within ± 0.070 GeV of the nominal K^{*0} mass. There is clear peaking of events near 1.4 GeV, indicating the presence of the $K_1(1400)$. (The $J/\psi \rightarrow K^{*0}\pi^\pm$ distribution of Fig. 12f should be compared with the corresponding distribution for ψ' decays shown in of Fig. 7f.)

5.2.1 Fits to the $J/\psi \rightarrow K^\pm\rho$ and $K^*\pi$ mass distributions.

To determine the number of $K_1(1270)$ events, we fit the $K\rho$ mass spectrum of Fig. 12c to $f_{K\rho}$ plus an s-wave Breit Wigner with the mass and width of the $K_1(1400)$ and an additional Breit Wigner with mass near 1.7 GeV and width near 0.3 GeV. We restrict the fit to $K\rho$ masses below 1.9 GeV. The resulting fit, shown in Fig. 13, gives an

96/04/22 11.00

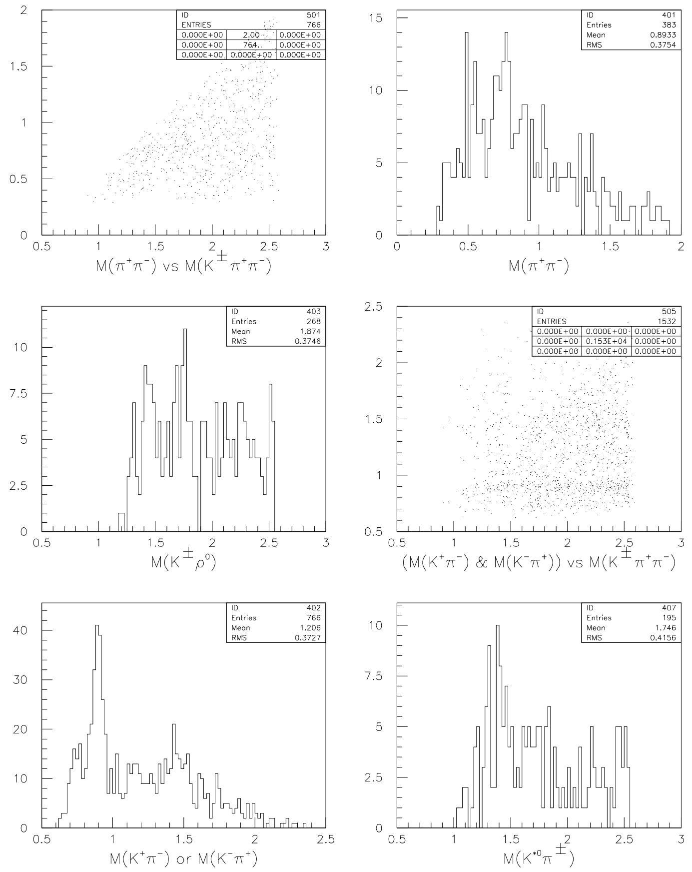

Figure 12: **a)** a) A scatterplot of $\pi^+\pi^-$ (vertical) vs $K^\pm\pi^+\pi^-$ (horizontal) masses for selected events. The **b)** $\pi^+\pi^-$ and **c)** K_ρ mass distributions. **d)** A scatterplot of $K^\pm\pi^\mp$ (vertical) vs $K^\pm\pi^+\pi^-$ (horizontal) masses for selected events. The **e)** $K\pi$ and **f)** $K^*\pi$ mass distributions.

8.3 ± 7.4 $K_1(1270)$ events, which we take as a 90% CL upper limit of $N^{(1270)}_{limit} < 17.8$ events.

The peak near $M_{K\rho} = 1.7$ GeV is well fit by a Breit Wigner with a mass and width that are reasonably well determined from the fit: $M = 1.78 \pm 0.02$ GeV and $\Gamma = 0.142 \pm 0.035$ GeV. These is consistent with the PDG values for the $K^*_3(1780)$, the strange member of the (3^-) octet, namely $M = 1.77 \pm 0.01$ GeV and $\Gamma = 0.164 \pm 0.017$ GeV [5].

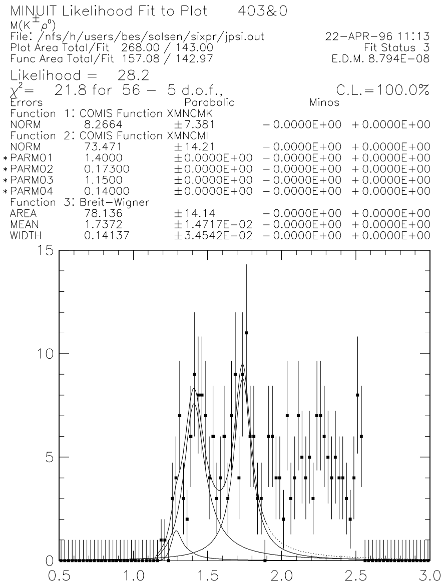

Figure 13: Fit to the $K^+\rho^0$ mass distribution using $f_{K\rho}$, an s-wave Breit Wigner with mass and width fixed at the PDG values for the $K_1(1400)$ and a Breit Wigner resonance with mass near 1.7 and width near 0.25 GeV.

We determine the number of $K_1(1400)$ events by applying a similar fit to the $K^*\pi$ mass spectrum of Fig. 12f. We keep the mass and width of the $K_1(1400)$ fixed at the PDG values and restrict the fit to $K^*\pi$ masses below 1.9 GeV. If we allow the mass and width of the $M \sim 1.7$ GeV Breit Wigner to vary, the resulting fit, shown in Fig. 14, gives 61.7 ± 17.0 $K_1(1400)$ events. If we repeat the fit with the width and mass of the $M \sim 1.7$ GeV Breit Wigner fixed at the values determined from the fit to the $K\rho$ mass spectrum, we find 79.2 ± 8.8 events. (Using the smooth background function f_{bkg} described above gives 74.6 ± 11.0 events, but with a rather poor confidence level.) We use the mean of these two results as the number of $K_1(1400)$ events and the difference from the mean as a systematic error: $N^{(1400)}_{K^*\pi} = 70.5 \pm 8.4 \pm 8.7$ events.

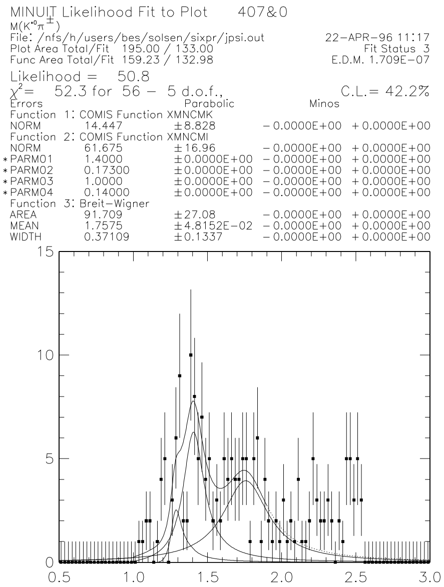

Figure 14: Fit to the $K^*\pi$ mass distribution using $f_{K\rho}$, an s-wave Breit Wigner with mass and width fixed at the PDG values for the $K_1(1400)$ and a Breit Wigner resonance with mass near 1.7 and width near 0.25 GeV.

5.3 $J/\psi \to K_1(1270)K$ and $K_1(1400)K$ branching ratio determination

5.3.1 $\psi' \to K_1^+K^-$ acceptance

The acceptance and the efficiency for the analysis cuts are evaluated by means of a sample of simulated Monte Carlo events. We generated 2000 $\psi' \to \pi^+\pi^- J/\psi; J/\psi \to K_1^+(1270)K^-$ with subsequent $K_1^+(1270) \to K^+\rho^0; \rho^0 \to \pi^+\pi^-$ decays with flat angular distributions. We also generated 2000 $\psi' \to \pi^+\pi^- J/\psi; J/\psi \to K_1^+(1400)K^-$ with subsequent $K_1^+(1400) \to K^{*0} \to K^+\pi^-$ decays, also with flat angular distributions. The generated events were passed through a Monte Carlo simulation of the BES detector that generates simulated detector responses. The simulated data are analyzed by the same programs that are used for the data. The K_ρ mass distribution for the events in the first sample that survive all the cuts is fit to the same $f_{K\rho}$ function, yielding 67.2 ± 8.4 events, or an acceptance for this mode of $\eta_{K\rho}^{(1270)} = 0.034 \pm 0.004$. The $K^*\pi$ mass distribution for the surviving events from the second sample are fit to an s-wave Breit Wigner function, yielding 62.5 ± 8.1 events, corresponding to an acceptance of $\eta_{K^*\pi}^{(1400)} = 0.031 \pm 0.004$. In the $K_1(1400) \to K^*\pi$ MC event sample, 40.3 ± 6.5 events have a $\pi^+\pi^-$ mass that is within ± 0.15 GeV of m_ρ, and pass the K_ρ

Table 3: A tabulation of the $J/\psi \to K_1 K$ selection cuts.

Numbers of events surviving each requirement

	94 data	95 data	Simulated events	
			$K_1(1270) \to K^+\rho^0$	$K_1(1400) \to K^{*0}\pi^+$
Preselection:				
Generated			2000	2000
6 chrgd trks			857	840
$\sum q = 0$	329720	612945	786	775
$\lvert\cos\theta_{chg}\rvert \leq 0.74$	155463	291948	332	295
$\chi^2_{4c} \leq 50$	459	824	183	159
Selection:				
$\chi^2_{5c} \leq 15$	205	345	123	110
$\lvert X^{K^+K^-}_{\pi K}\rvert > 0.1$	146	237	90	80
Mass cuts:				
$\lvert M_{\pi^+\pi^-} - M_\rho\rvert \leq 0.15$GeV	50	84	64	35
$\lvert M_{K\pi} - M_{K^*}\rvert \leq 0.07$GeV	68	127	37	65

selection requirements. We infer from this an acceptance for $K_1(1270) \to K^*\pi$ decays $\eta^{(1270)}_{K^*\pi} = 0.020 \pm 0.003$. A summary of the effect of the cuts on the real and simulated data is provided in Table 3.

5.3.2 J/ψ branching ratio results

We determine the 90% CL upper limit for $Br(J/\psi \to K_1^+(1270)K^- \ + \ cc)$ using the relation given in eqn. 18, above, with the additional factor of $Br(\psi' \to \pi^+\pi^- J/\psi) = 0.324 \pm 0.026$ [5] in the denominator. The resulting limit of

$$Br(J/\psi \to K_1^+(1270)K^- \ + \ cc) < 1.8 \times 10^{-3} \ \ 90\% \text{ CL} \tag{22}$$

is more than a factor of two below the result expected from applying the 14% rule to our result for ψ' decays to this channel.

We use the relation given in eqn. 20, with $Br(\psi' \to \pi^+\pi^- J/\psi)$ included in the denominator, to determine a branching fraction for $J/\psi \to K_1^+(1400)K^-$. Our result,

$$Br(J/\psi \to K_1^+(1400)K^- \ + \ cc) = (5.0 \pm 0.6 \pm 1.1) \times 10^{-3}, \tag{23}$$

is well above our upper limit for the $K_1(1270)\overline{K}$ mode, indicating a flavor-SU(3) violation in J/ψ decays that is opposite to that seen in ψ' decays. Attempts to accomodate this effect in J/ψ decays by adjusting the K_A-K_B mixing angle will exacerbate the violation in the ψ' decays.

6 Summary

We have measured the $\psi' \rightarrow AP$ decay branching ratios

- $Br(\psi' \rightarrow b_1^+\pi^- \ + \ cc) = (6.6 \pm 0.8 \pm 1.4) \times 10^{-4}$;
- $Br(\psi' \rightarrow K_1^+(1270)K^- \ + \ cc) = (7.6 \pm 0.9 \pm 1.5) \times 10^{-4}$; and
- $Br(\psi' \rightarrow K_1^+(1400)K^- \ + \ cc) < 2.7 \times 10^{-4}$ 90% CL.

We find that AP decays are dominant exclusive hadron channels for the ψ'. The discrepancy between the $K_1(1270)$ and $K_1(1400)$ rates is contrary to expectations based on flavor-SU(3).

We have made a first measurement of J/ψ decays to strange AP final states:

- $Br(J/\psi \rightarrow K_1^+(1270)K^- \ + \ cc) < 1.8 \times 10^{-3}$ 90% CL and
- $Br(J/\psi \rightarrow K_1^+(1400)K^- \ + \ cc) = (5.0 \pm 0.6 \pm 1.1) \times 10^{-3}$.

The $K_1(1270)\overline{K}$ channel is the first observation of an exclusive ψ' hadronic decay channel that is enhanced relative to the J/ψ in the context of the 14% rule. In addition, the flavor-SU(3)-violating $K_1(1270)$-$K_1(1400)$ asymmetry has an opposite character for the ψ' and J/ψ. This can not be accommodated by adjustments of the singlet-triplet mixing angle.

7 Acknowledgements

I acknowledge the patient help and assistance of Yifan Gu and the members of the BES ψ' analysis groups at IHEP and the University of Hawaii. All of the Monte Carlo event samples used in this analysis were prepared by Lingjun Pan. Josephine Bolosan and Fred Harris gave me considerable help in recovering from a unix-related disaster that I encountered during the preparation of this report. This research is supported by the U.S. Department of Energy research grant number DE-FG03-94ER40833.

References

[1] M.E.B. Franklin *et al.* (Mark II Collaboration), Phys. Rev. Lett. **51**, 963 (1983).

[2] J.Z. Bai *et al.* (BES Collaboration), *Search for $\psi' \to$ Vector + Pseudoscalar Decays*, paper submitted to the 1995 International Symposium on Lepton and Photon Interactions at High Energies, Beijing, China.

[3] J.Z. Bai *et al.* (BES Collaboration), *Observation of New Anomalous Charmonium Decays*, paper submitted to the 1995 International Symposium on Lepton and Photon Interactions at High Energies, Beijing, China.

[4] See, for example, H.G. Blundell, S. Godfrey, and B. Phelps, Phys. Rev. **53**, 3712 (1996), M. Suzuki, Phys. Rev. **D47**, 1252 (1993), and references cited therein.

[5] L. Montanet *et al.* (Particle Data Group), Phys. Rev. **D50**, 1173 (1994).

[6] J.Z. Bai *et al.* (BES Collaboration), Nucl. Instr. and Meth. **A344**, 319 (1994) and Phys. Rev. Lett. **69**, 3021 1992.

[7] J.Z. Bai *et al.* (BES Collaboration), *Branching Fractions for ψ' Decays to Octet-Baryon Pairs*, paper submitted to the 1995 International Symposium on Lepton and Photon Interactions at High Energies, Beijing, China.

[8] W.M. Dunwoodie, private communication.